*Acta Cryst.* (1974). B30, 853

# The Crystal Structure of $Mo_6Ga_{31}$, a Hypersymmetrical Structure Solved by Direct Methods

BY K. YVON

*Laboratoire de Cristallographie aux Rayons X de l'Université, 32 Bd. d'Yvoy, CH-1211 Genève, Switzerland*

(*Received* 26 *September* 1973; *accepted* 22 *November* 1973)

$Mo_6Ga_{31}$ is monoclinic and crystallizes in a new structure type: $a=9{\cdot}517$ (3), $b=16{\cdot}067$ (4), $c=16{\cdot}995$ (5) Å, $\beta=95{\cdot}09$ (2)°, space group $P2_1/c$, $Z=4$, $D_x=7{\cdot}0$ g cm$^{-3}$ (single-crystal diffractometry, refinement by the least-squares method, $R_{|F|>4\sigma}=6\%$). The most important structural features are $MoGa_{10}$ polyhedra arranged at the corners of distorted cubes and gallium layers penetrating the crystal structure in different directions. There are no Mo–Mo contacts, no Ga–Ga pairs but some very short Mo–Ga distances. Not all sites have full occupancy, suggesting that the '$MoGa_5$-phase' has a range of homogeneity between the limits $Mo_6Ga_{31}$ and $Mo_7Ga_{30}$. This crystal structure is compared with other complex structures of transition metal gallides and aluminides. In order to solve the crystal structure by use of direct methods renormalization of the structure factors was necessary.

## Introduction

It is surprising still to find binary systems of metallic compounds on which practically no X-ray examinations have been carried out. Such is the case for the molybdenum–gallium system, whose phase diagram was only recently published (Bornand, Siemens & Oden, 1973). It gives the approximate stoichiometry and decomposition temperature for two intermetallic compounds: $Mo_3Ga$ and $MoGa_5$. $Mo_3Ga$ crystallizes with the $\beta$-W type structure ($A15$), which is a structure of considerable interest for low-temperature physicists. Compounds with this structure have superconducting transition temperatures that depend strongly on the valence electron concentration (v.e.c.) and range from $<1$ up to 22 °K, the highest value measured so far.

The search for superconductors with high transition temperatures revealed the existence of a Ga-rich phase, which was first denoted '$MoGa_4$' (Matthias, Compton & Corenzwit, 1961) but corresponds to the $MoGa_5$ phase mentioned above. X-ray powder analysis suggested that this compound has a rather complex crystal structure. It was therefore surprising to find relatively high superconducting transition temperatures between 8 and 9 °K. Of even greater interest however was the magnetic behaviour at low temperatures. $MoGa_5$ is diamagnetic, having a critical field $H_{c_2}$ of 74 kG (Fischer, 1972). Moreover, by dissolving very small amounts of 'magnetic impurities' like Mn in the crystal structure, anomalous values of the magnetic moment ('giant moments') of 7·5 B.M. per atom were observed and experimental evidence for the 'internal compensation effect' predicted by Jaccarino & Peter was obtained (Jaccarino & Peter, 1962; Fischer, Jones, Bongi, Frei & Treyvaud, 1971). In order to continue with theoretical calculations on these findings, the knowledge of the exact composition and the environment of the transition element in this compound is of importance. It became, therefore highly desirable to solve its crystal structure. The reasons for such an investigation not having been carried out up to this time are the difficulties of obtaining single crystals suitable for X-ray examination and the very particular crystal structure of $MoGa_5$ which has resisted standard methods of X-ray structure analysis. The failure to obtain good single crystals was partly due to the absence of an accurate phase diagram indicating the temperature and composition range of the $MoGa_5$ phase.

It was therefore decided to perform a preliminary X-ray study on the entire Mo–Ga system in order to gain insight into the phase relations.

## Sample preparation

High purity gallium was added to molybdenum powder ($<10\mu$m) in compositions covering the entire range of the phase diagram. The samples were heated in alumina crucibles up to 1100 °C under 1 atm of pure argon and held at this temperature until all the molybdenum powder was dissolved in the melt. Then the temperature was slowly lowered until the melt solidified. During this procedure, curious phenomena were observed with samples in the composition range between $MoGa_4$ and $MoGa_6$. At temperatures of about 700 °C, the melt suddenly increased substantially in volume, decomposing into a very fine and loosely-packed powder at lower temperatures. A similar observation seems to have been made in the Pt–Al system (Edshammar, 1966). In order to interpret this phenomenon, it is attractive to speculate on the formation of Mo–Ga clusters in the melt at temperatures close to solidification (see last paragraph).

## X-ray powder analysis

The two prominent phases $Mo_3Ga$ and $MoGa_5$ form very quickly and are readily recognizable on powder photographs. $Mo_3Ga$ ($\beta$-tungsten type, $A15$, $a=4{\cdot}94$ Å) gives few and very sharp lines, whereas $MoGa_5$ has a

very complex powder pattern characterized by many diffuse reflexion bands (Table 1). Guinier photographs suggested that this phase might have a homogeneity range between $MoGa_{4.5}$ and $MoGa_{5.5}$. There was practically no change in the powder pattern over this range of composition, indicating that substitution of Mo and Ga atoms in the crystal structure was probable ($r_{Ga}$ = 1·41, $r_{Mo}$ = 1·40 Å).*

Table 1. *Powder pattern of the* $MoGa_5$ *phase*, Cu $K\alpha$, $I_{calc}$ *contains the Lp factor for a Guinier camera using a quartz monochromator*

*vw*: very weak, *w*: weak, *m*: medium, *s*: strong, *vs*: very strong *diff*: diffuse.

Only observed reflexions are included in the list.

| $h$ | $k$ | $l$ | $d$(Å) | $I_{obs}$ | $I_{calc}$ |
|---|---|---|---|---|---|
| 0 | 2 | 3 | 4·62 | *vw* | 100 |
| 2 | 2 | −1 | 4·04 | *vs* | 461 |
| 1 | 2 | 3 | 4·04 | | 461 |
| 0 | 4 | 0 | 4·02 | *s* | 220 |
| 1 | 0 | −4 | 4·00 | *s* | 207 |
| 3 | 0 | 2 | 2·88 | *s* | 326 |
| 1 | 4 | −4 | 2·83 | *m, diff* | 452 |
| 3 | 1 | 3 | 2·62 | *w, diff* | 118 |
| 2 | 5 | 1 | 2·61 | | 108 |
| 2 | 4 | −4 | 2·55 | *m, diff* | 320 |
| 3 | 4 | 2 | 2·34 | | 263 |
| 2 | 0 | 6 | 2·34 | *s* | 188 |
| 0 | 5 | 5 | 2·33 | | 127 |
| 2 | 6 | −1 | 2·32 | | 259 |
| 1 | 6 | 3 | 2·32 | *s* | 192 |
| 3 | 2 | −5 | 2·32 | | 226 |
| 0 | 2 | 7 | 2·32 | | 167 |
| 1 | 5 | −5 | 2·30 | *m* | 599 |
| 1 | 2 | −7 | 2·30 | | 251 |
| 4 | 2 | −1 | 2·28 | *m* | 241 |
| 1 | 5 | 5 | 2·23 | *m* | 178 |
| 4 | 0 | 2 | 2·23 | | 364 |
| 0 | 7 | 2 | 2·215 | | 298 |
| 3 | 5 | 1 | 2·215 | | 131 |
| 2 | 1 | −7 | 2·215 | *s, diff* | 102 |
| 3 | 3 | 4 | 2·213 | | 171 |
| 3 | 4 | −4 | 2·210 | | 219 |
| 1 | 4 | 6 | 2·206 | | 535 |
| 4 | 3 | −1 | 2·172 | | 187 |
| 1 | 7 | −2 | 2·168 | *m, diff* | 205 |
| 4 | 3 | 0 | 2·167 | | 227 |
| 2 | 2 | −7 | 2·154 | *w* | 299 |
| 3 | 5 | −3 | 2·140 | *m, diff* | 245 |
| 3 | 2 | 5 | 2·135 | | 249 |
| 2 | 6 | 3 | 2·122 | *vw* | 117 |
| 4 | 1 | 3 | 2·101 | *vw* | 89 |
| 1 | 5 | −6 | 2·099 | | 91 |
| 4 | 4 | −2 | 2·020 | *vs* | 962 |
| 2 | 4 | 6 | 2·019 | | 1000 |
| 0 | 8 | 0 | 2·008 | *s* | 514 |
| 2 | 0 | −8 | 2·000 | *s* | 397 |
| 4 | 2 | −5 | 1·966 | *vw* | 60 |
| 1 | 8 | 0 | 1·965 | | 66 |

A list of the $d$ values for most of the strong reflexions as well as their observed and calculated intensities is given in Table 1. Owing to overlap, accurate lattice parameters could not be derived from powder photographs. The following values were obtained from several single crystals measured on the automatic diffractometer: $a$ = 9·517 (3), $b$ = 16·067 (4), $c$ = 16·995 (5) Å, $\beta$ = 95·09 (2)°. The experimental density was measured by displacement: $\varrho$ = 7·0 (1) g cm$^{-3}$.

### Preparation of single crystals

Samples in the composition range between $MoGa_4$ and $MoGa_6$ usually do not contain single crystals large enough for X-ray analysis. This is a consequence of the previously described anomaly of the melt yielding a powder of an estimated average grain size of a few microns. Annealing did not result in a substantial increase of this grain size, so that we tried to obtain single crystals in more gallium-rich samples.

One such sample contained well developed needles suitable for single-crystal analysis. It is difficult to state exact experimental conditions for growing these crystals, since they probably form only in a very restricted range of concentration ($\sim MoGa_5$) and of temperature ($\sim$ 700 °C). These single crystals have $2/m$ symmetry, the needle axis corresponding to **a**. Precession photographs indicated the space group $P2_1/c$, the systematic extinctions being for $h0l$: $l = 2n+1$ and for $0k0$: $k = 2n+1$.

### Data collection

Complete data sets of four different crystals were collected with an automatic single-crystal diffractometer (Philips PW1100) using $\omega$–$2\theta$ scans and Mo $K\alpha$ radiation (graphite monochromator). The largest crystal (400 × 50 × 50 $\mu$m) was used for collecting very quickly most intensities in the Mo sphere (about 13000 independent reflexions). Such a relatively large number of data were measured in order to find a sufficiently great number of strong reflexions necessary for successful application of statistical methods. Owing to the very

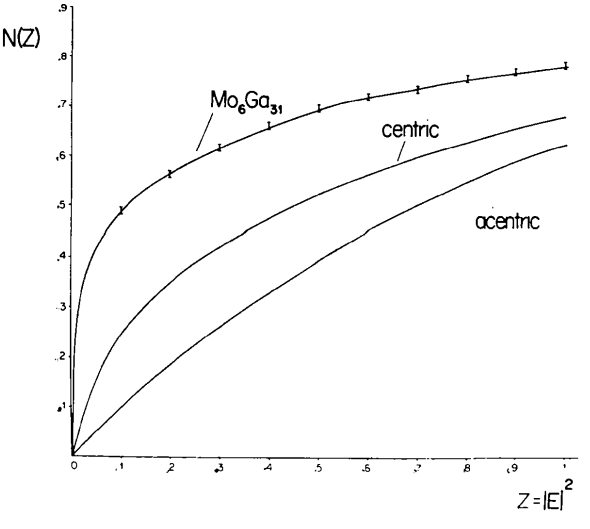


Fig. 1. Theoretical $N(z)$ curves and experimental distribution of normalized structure factors for $MoGa_5$.

* Metallic radii for coordination 12 compiled by Teatum, Gschneidner and Waber (Pearson, 1972).

special distribution of X-ray intensities of $MoGa_5$, an abnormally large fraction of reflexions had intensities too low for use by these methods.

Data sets for the other crystals of smaller size ($25 \times 25 \times 200$ $\mu$m) were collected with higher precision and kept for later refinement of structure parameters. $|F|$ values and their standard deviations were calculated as usual and small intensities were treated as follows:

if $|F|^2 < \sigma_{|F|^2}$, $|F|^2$ was replaced by $\frac{1}{2}(|F|^2 + \sigma_{|F|^2})$.

Correction for absorption ($\mu_{MoGa_5} = 370$ cm$^{-1}$) was made applying the analytical method (de Meulenaer & Tompa, 1965) and using a computer program written by Tompa & Alcock (1969). The transmission factors varied between 0·27 and 0·18.

### The $|F|^2$ synthesis for $MoGa_5$

A three-dimensional $|F|^2$ synthesis was calculated for 250 000 grid points using 4500 independent reflexions. It was surprising to find that despite the large number of about 150 atoms per unit cell, this map nevertheless revealed interesting features useful for the structure determination. Besides two prominent Harker peaks at (0, 0·26, 0·5) and (0·87, 0·5, 0·30) about 60 peaks had heights that were greater than 10% of the origin peak. This can only be explained by the presence of a large number of equal interatomic vectors in the crystal structure. About half of all strong peaks were located on, or very close to, positions that could be attributed to a cubic cell with $a = 5{\cdot}76$ Å. This cell was especially well visible in the four zones {102}, {301}, {872}, {8$\bar{7}$2} corresponding to the directions of the body diagonals in this cube. Approximate threefold symmetry is visible in these sections, but not so in upper layers. This cubic cell can therefore be only a very crude approximation to the substructure of $MoGa_5$. Furthermore, many high peaks in the $|F|^2$ map still remained uninterpreted and it finally turned out to be impossible to proceed any further by use of Patterson methods alone. Current methods like superposition

Table 2. *Atomic fractional coordinates* ($\times 10^4$), *occupancy factors and their least-squares values* $d(\times 10^2)$, *an thermal parameters* ($\times 10^2$) *with their standard deviations in brackets, for* $Mo_6Ga_{31}$, *space group* $P2_1/c$ (*No.* 14)

All atoms are in equipoint 4(*e*) except for Ga(31) in 2(*a*) and Ga(32) in 2(*c*).

| | *x* | *y* | *z* | Occupancy | | $B$(Å$^2$) |
|---|---|---|---|---|---|---|
| Ga(1) | 180 (8) | 2456 (5) | 122 (5) | 1·0 | 102 (4) | 85 (15) |
| Ga(2) | 7234 (8) | 2008 (5) | 194 (4) | 1·0 | 102 (3) | 111 (14) |
| Ga(3) | 6992 (9) | 28 (6) | 418 (5) | 0·9 | 90 (3) | 158 (15) |
| Ga(4) | 6273 (6) | 3844 (6) | 471 (3) | 1·0 | 101 (3) | 75 (12) |
| Ga(5) | 4592 (9) | 850 (5) | 735 (5) | 0·9 | 91 (3) | 141 (15) |
| Ga(6) | 2812 (9) | 2562 (6) | 913 (5) | 1·0 | 100 (3) | 102 (16) |
| Ga(7) | 9106 (7) | 3791 (6) | 1073 (4) | 1·0 | 99 (3) | 100 (13) |
| Ga(8) | 9508 (8) | 1218 (6) | 1077 (5) | 1·0 | 99 (3) | 90 (13) |
| Ga(9) | 5643 (9) | 2488 (6) | 1381 (5) | 1·0 | 99 (3) | 78 (14) |
| Ga(10) | 1669 (7) | 3845 (6) | 1836 (4) | 1·0 | 99 (3) | 73 (12) |
| Ga(11) | 2223 (8) | 1351 (5) | 1927 (4) | 1·0 | 100 (3) | 94 (16) |
| Ga(12) | 8439 (9) | 2416 (5) | 2041 (5) | 1·0 | 102 (4) | 64 (16) |
| Ga(13) | 8907 (9) | 33 (5) | 2091 (5) | 1·0 | 101 (4) | 75 (15) |
| Ga(14) | 6580 (6) | 3841 (6) | 2400 (4) | 1·0 | 103 (2) | 97 (11) |
| Ga(15) | 5026 (9) | 1309 (6) | 2486 (5) | 1·0 | 98 (3) | 89 (13) |
| Ga(16) | 4014 (9) | 2955 (5) | 2748 (5) | 1·0 | 100 (3) | 121 (15) |
| Ga(17) | 4044 (8) | 4702 (5) | 2813 (5) | 1·0 | 101 (3) | 106 (14) |
| Ga(18) | 1066 (9) | 2566 (6) | 2875 (5) | 1·0 | 98 (4) | 79 (15) |
| Ga(19) | 1563 (9) | 204 (5) | 3035 (5) | 1·0 | 100 (3) | 96 (15) |
| Ga(20) | 7954 (8) | 1210 (6) | 3086 (4) | 1·0 | 100 (3) | 81 (14) |
| Ga(21) | 4396 (8) | 203 (5) | 3641 (5) | 1·0 | 99 (3) | 80 (14) |
| Ga(22) | 8222 (8) | 2859 (5) | 3663 (5) | 1·0 | 98 (3) | 98 (15) |
| Ga(23) | 7986 (8) | 4729 (5) | 3681 (4) | 1·0 | 101 (3) | 102 (14) |
| Ga(24) | 707 (9) | 3804 (6) | 3983 (5) | 1·0 | 100 (2) | 90 (11) |
| Ga(25) | 5686 (9) | 1959 (4) | 4019 (5) | 1·0 | 102 (3) | 95 (11) |
| Ga(26)* | 5641 (9) | 3846 (6) | 4022 (5) | 1·0 | 98 (2) | 121 (10) |
| Ga(27) | 740 (8) | 1328 (5) | 4049 (5) | 1·0 | 97 (3) | 91 (14) |
| Ga(28) | 7317 (9) | 51 (5) | 4200 (5) | 1·0 | 97 (3) | 75 (15) |
| Ga(29) | 3271 (7) | 2971 (5) | 4341 (4) | 1·0 | 104 (3) | 103 (13) |
| Ga(30) | 3459 (7) | 1224 (6) | 4890 (6) | 1·0 | 99 (3) | 72 (12) |
| Ga(31) | 0 | 0 | 0 | 1·0 | 96 (4) | 62 (23) |
| Ga(32) | 0 | 5000 | 0 | 0·9 | 90 (4) | 166 (27) |
| Mo(1) | 1848 (6) | 1131 (4) | 403 (3) | 1·0 | 100 | 39 (9) |
| Mo(2) | 4247 (5) | 3839 (4) | 1409 (3) | 1·0 | 98 (2) | 24 (7) |
| Mo(3) | 7000 (6) | 1109 (4) | 1566 (3) | 1·0 | 98 (2) | 10 (10) |
| Mo(4) | 9378 (5) | 3819 (4) | 2619 (3) | 1·0 | 97 (2) | 20 (8) |
| Mo(5) | 3092 (6) | 1585 (4) | 3395 (3) | 1·0 | 97 (2) | 43 (10) |
| Mo(6) | 8299 (6) | 1489 (4) | 4606 (3) | 1·0 | 97 (2) | 44 (11) |

* The site Ga(26) in $Mo_7Ga_{30}$ is probably occupied by molybdenum.

minimum functions, image seeking or vector verification all suffer from the annoying presence of multiply superposed peaks and often fail to solve hypersymmetrical crystal structures at all. Therefore, an attempt was made to use statistical methods.

### Calculation of normalized structure factors

Owing to the presence of building blocks in the structure of $MoGa_5$, many regions of $\sin\theta/\lambda$ had abnormally high intensity averages. This had been recognized on powder patterns where many of the strongest intensities are grouped around $d$ values of 2 and 4 Å. It was therefore difficult to derive scale and temperature factors from a Wilson plot. An overall temperature factor of $B=1{\cdot}0$ Å$^2$ was finally used for calculation of the normalized structure factors and the scale factor was fixed by imposing the condition $\langle E^2_{hkl}\rangle = 1{\cdot}0$. An $N(Z)$ plot (Fig. 1) revealed that the distribution of structure factors for $MoGa_5$ is 'hypersymmetric' (Rogers & Wilson, 1953).

### Renormalization

Several attempts to use this original set of $|E|$ values for statistical methods failed to yield the correct structure. This was due to the presence of the previously mentioned building blocks. Such sub-units usually give rise to a non-Gaussian distribution of structure factors and violate the assumption of randomness under which probability formulae of sign determination are derived. From inspection of the $|F|^2$ synthesis it was concluded that the most likely structure of these sub-units might correspond to the atom arrangement in the $NiHg_4$ type [space group $Im3m$, 2Mo in ($a$), 8 Ga in ($c$): Bauer, Nowotny & Stempfl (1953)].

In order to account for these sub-units, renormalization of the $|E|$ values was necessary (Hauptman & Karle, 1959; Hauptman, 1964). This was done by subtracting the contribution of the subcell from the observed intensities and by recalculating normalized structurefactors with this new set of corrected intensities. The final set of renormalized structure factors used in the symbolic addition method contained 336 $|E|$ values greater than 1·5.

### Symbolic addition

After generating about 4000 triple-product sign relationships by use of the computer program *LSAM* (Main, Woolfson, Germain, 1972) three reflexions were chosen in order to define the origin in the unit cell according to the known selection rules. Owing to the presence of building blocks in the structure, care had to be taken not to select more than one reflexion out of the subset of structure factors corresponding to the cubic cell used for renormalizing the $|E|$ values. The following reflexions were used:

| | |
|---|---|
| 1,2,13, 3,13,$\bar{3}$, 146 | (origin) |
| 5,4,$\bar{12}$, 5,17,3, 10,6,$\bar{1}$, 4,17,$\bar{17}$ | (symbols $a,b,c,d$). |

The symbolic addition procedure resulted in multiple solutions of which the ones with the highest figures of merit were used for calculating $|E|$ maps. One of them (the fourth best) contained essentially the correct structure. This was not immediately realized, however, for the following reasons. Firstly, the exact number of atoms expected in the asymmetric unit was not known, since the specific gravity of $MoGa_5$ could only be measured with low accuracy. Secondly, the amplitude termination effects (Burgi & Dunitz, 1971) in $|E|$ maps of hypersymmetrical crystal structures result inevitably in 'ghost-peaks' making it often difficult to sort out correct atom positions. The third and most discouraging difficulty was the fact that the conventional $R$ values calculated for all the different solutions obtained from the statistical methods were practically identical and always very close to the theoretical values of a 'completely wrong' structure. Even during the initial refinement of the correct structure model by $F_o$ syntheses, this $R$ value did not drop significantly, so that considerable computational effort was necessary to recognize which set of $|E|$ values gave a refinable electron-density map and which did not. This was finally achieved with set 4 at an $R$ value of 55%. Successive refinement by electron-density methods resulted in the recognition of 38 atomic sites per asymmetric unit. Throughout this procedure weighted Fourier coefficients were used (Woolfson, 1970).

### Refinement of the structure

Refinement of the structure by $F_o$ and $\Delta F$ syntheses was slow and did not reduce the convential $R$ value below 20%. Least-squares methods gave better convergence by comparison, but suffered from the presence of strong parameter correlations and from partially occupied sites. Therefore, occupancy factors and positional as well as thermal parameters had to be refined in separate stages. The full-matrix least-squares program *ORXFLS*3 (Busing *et al.*, 1971*b*) was used and correction for extinction and anomalous dispersion was made ($g'=0{\cdot}0003$; Ga: $\Delta f'=0{\cdot}2$, $\Delta f''=1{\cdot}7$; Mo: $\Delta f'=-1{\cdot}7$, $\Delta f''=0{\cdot}9$).

Atomic scattering factors were taken from *International Tables for X-ray Crystallography* (1962). The weighting scheme $w=1/\sigma^2$ was applied and refinement was considered complete when the last shifts of the parameters were 0·1 of their estimated standard deviations (e.s.d.). The final 184 parameters and their e.s.d.'s are listed in Table 2. The residual $R=\sum\Delta F_o/\sum|F_o|$ is 6% for 1500 reflexions with $|F|>4\sigma$ and 10% for 3200 reflexions with $|F|>\sigma$. A list of observed and calculated structure factors is given in Table 4. A final difference electron-density map revealed no abnormal features and confirmed the partial occupancies of the four atom sites.

### Composition of $MoGa_5$

Refinement of the occupancy factors for the 38 different atomic sites revealed that at least 6 of them are occupied by molybdenum atoms and that many sites have more or less pronounced defect character. Especially one site ($x,y,z \equiv 0{\cdot}564$, 0·385, 0·402), originally identified as an Mo atom, had an occupancy that corresponded to a gallium atom rather than to a partially occupied Mo. This assumption is supported by the interatomic distances from this atom to those coordinating it. They are significantly larger than the Mo–Ga distances observed in other coordination shells and correspond rather to Ga–Ga distances (Table 3).

Table 3. *Interatomic distances and coordination number*

(*a*) Interatomic distances (Å), with e.s.d.'s, for $Mo_6Ga_{31}$. Included are all Mo–Ga distances less than 4 Å.

| | | | |
|---|---|---|---|
| Mo(1)–Ga(24) | 2·559 (12) | Mo(4)–Ga(24) | 2·541 (11) |
| Ga(31) | 2·579 (7) | Ga(13) | 2·563 (11) |
| Ga(6) | 2·596 (13) | Ga(12) | 2·587 (11) |
| Ga(8) | 2·596 (11) | Ga(18) | 2·588 (12) |
| Ga(11) | 2·607 (11) | Ga(19) | 2·609 (11) |
| Ga(3) | 2·629 (13) | Ga(7) | 2·617 (10) |
| Ga(5) | 2·661 (12) | Ga(10) | 2·654 (9) |
| Ga(1) | 2·672 (12) | Ga(14) | 2·656 (8) |
| Ga(23) | 2·735 (11) | Ga(22) | 2·661 (11) |
| Ga(29) | 2·758 (11) | Ga(23) | 2·752 (10) |
| Mean value: 2·639 | | Mean value: 2·623 | |
| Mo(2)–Ga(21) | 2·547 (11) | Mo(5)–Ga(15) | 2·544 (11) |
| Ga(9) | 2·548 (12) | Ga(21) | 2·561 (11) |
| Ga(6) | 2·566 (12) | Ga(11) | 2·584 (10) |
| Ga(4) | 2·607 (9) | Ga(18) | 2·585 (12) |
| Ga(28) | 2·609 (11) | Ga(30) | 2·600 (10) |
| Ga(10) | 2·620 (9) | Ga(27) | 2·619 (11) |
| Ga(30) | 2·626 (9) | Ga(16) | 2·644 (12) |
| Ga(14) | 2·665 (9) | Ga(25) | 2·667 (12) |
| Ga(16) | 2·709 (11) | Ga(19) | 2·694 (12) |
| Ga(17) | 2·781 (11) | Ga(29) | 2·744 (11) |
| Mean value: 2·628 | | Mean value: 2·624 | |
| Mo(3)–Ga(15) | 2·568 (11) | Mo(6)–Ga(1) | 2·562 (11) |
| Ga(9) | 2·569 (12) | Ga(28) | 2·565 (11) |
| Ga(12) | 2·595 (11) | Ga(7) | 2·583 (11) |
| Ga(8) | 2·603 (11) | Ga(4) | 2·583 (9) |
| Ga(13) | 2·607 (11) | Ga(27) | 2·598 (11) |
| Ga(3) | 2·612 (12) | Ga(20) | 2·614 (11) |
| Ga(5) | 2·617 (12) | Ga(25) | 2·704 (12) |
| Ga(20) | 2·666 (10) | Ga(22) | 2·720 (11) |
| Ga(17) | 2·720 (11) | Ga(2) | 2·834 (11) |
| Ga(2) | 2·769 (11) | Ga(32) | 2·933 (7) |
| Mean value: 2·633 | | Mean value: 2·670 | |
| Ga(26)*–Ga(23) | 2·751 (13) | | |
| Ga(29) | 2·752 (13) | | |
| Ga(2) | 2·759 (14) | | |
| Ga(17) | 2·806 (14) | | |
| Ga(16) | 2·923 (15) | | |
| Ga(14) | 2·972 (12) | | |
| Ga(22) | 3·031 (13) | | |
| Ga(25) | 3·032 (13) | | |
| Ga(3) | 3·166 (15) | | |
| Ga(5) | 3·197 (15) | | |
| Ga(5) | 3·257 (15) | | |
| Ga(3) | 3·348 (14) | | |
| Mean value: 3·000 | | | |

* The site Ga(26) may also be occupied by molybdenum.

Table 3 (*cont.*)

(*b*) Coordination number (CN) for the Ga atoms in $Mo_6Ga_{31}$ and number of Mo and Ga atoms ($n_{Mo}, n_{Ga}$) within a sphere of 3·5 Å around each Ga atom. The shortest Ga–Ga contact, $d_{min}$(Ga–Ga) (Å), is given for each polyhedron.

| | CN | $n_{Mo}$ | $n_{Ga}$ | $d_{min}$(Ga–Ga) |
|---|---|---|---|---|
| Ga(1) | 10 | 2 | 8 | 2·680 |
| Ga(2) | 12 | 2 | 10 | 2·739 |
| Ga(3) | 14 | 2 | 12 | 2·732 |
| Ga(4) | 10 | 2 | 8 | 2·759 |
| Ga(5) | 14 | 2 | 12 | 2·732 |
| Ga(6) | 10 | 2 | 8 | 2·693 |
| Ga(7) | 9 | 2 | 7 | 2·660 |
| Ga(8) | 10 | 2 | 8 | 2·664 |
| Ga(9) | 10 | 2 | 8 | 2·739 |
| Ga(10) | 9 | 2 | 7 | 2·660 |
| Ga(11) | 10 | 2 | 8 | 2·693 |
| Ga(12) | 10 | 2 | 8 | 2·696 |
| Ga(13) | 10 | 2 | 8 | 2·664 |
| Ga(14) | 13 | 2 | 11 | 2·837 |
| Ga(15) | 10 | 2 | 8 | 2·752 |
| Ga(16) | 13 | 2 | 11 | 2·810 |
| Ga(17) | 12 | 2 | 10 | 2·789 |
| Ga(18) | 10 | 2 | 8 | 2·773 |
| Ga(19) | 9 | 2 | 7 | 2·661 |
| Ga(20) | 10 | 2 | 8 | 2·696 |
| Ga(21) | 10 | 2 | 8 | 2·753 |
| Ga(22) | 13 | 2 | 11 | 2·821 |
| Ga(23) | 13 | 2 | 11 | 2·751 |
| Ga(24) | 10 | 2 | 8 | 2·710 |
| Ga(25) | 13 | 2 | 11 | 2·797 |
| Ga(26) | 12 | – | 12 | 2·751 |
| Ga(27) | 9 | 2 | 7 | 2·661 |
| Ga(28) | 9 | 2 | 7 | 2·707 |
| Ga(29) | 12 | 2 | 10 | 2·752 |
| Ga(30) | 9 | 2 | 7 | 2·707 |
| Ga(31) | 10 | 2 | 8 | 2·710 |
| Ga(32) | 8 | 2 | 6 | 2·785 |

Analysis of the single crystal by a microprobe* indicated a composition of $MoGa_{5\cdot1\pm0\cdot1}$, which is in good agreement with the formula $Mo_6Ga_{31}$. It is however likely that $MoGa_5$ has a domain of homogeneity between $Mo_6Ga_{31}$ and $Mo_7Ga_{30}$, and that the change in composition over this range is conditioned by gradually replacing one molybdenum atom by one gallium atom.

In order to find evidence for this assumption, data sets of different crystals were refined, in the hope that the occupancy factor of the site with occupational disorder [Ga(26)] might change. The result, however, was negative. This is certainly related to the fact that large needles form peritectically only in a small concentration and temperature range at the Ga-rich limit of the phase, and therefore always have the composition $Mo_6Ga_{31}$.

There is, however, one additional detail worth mentioning: comparison of the powder diffraction patterns of samples $Mo_6Ga_{31}$ and $Mo_7Ga_{30}$ with the calculated intensities (Yvon, Jeitschko & Parthé, 1969) revealed some small discrepancies. This indicates that

* These analyses were carried out by M Burri, Institut de Physique Expérimentale, Université de Lausanne and M Bertrand, Département de Minéralogie, Université de Genève.

Table 4. *Observed and calculated structure factors for* $Mo_6Ga_{31}$

The columns contain from left to the right: $k$, $l$, $F_{obs}$, $F_{calc}$. Only reflexions with $|F| > 4\sigma$ are included.

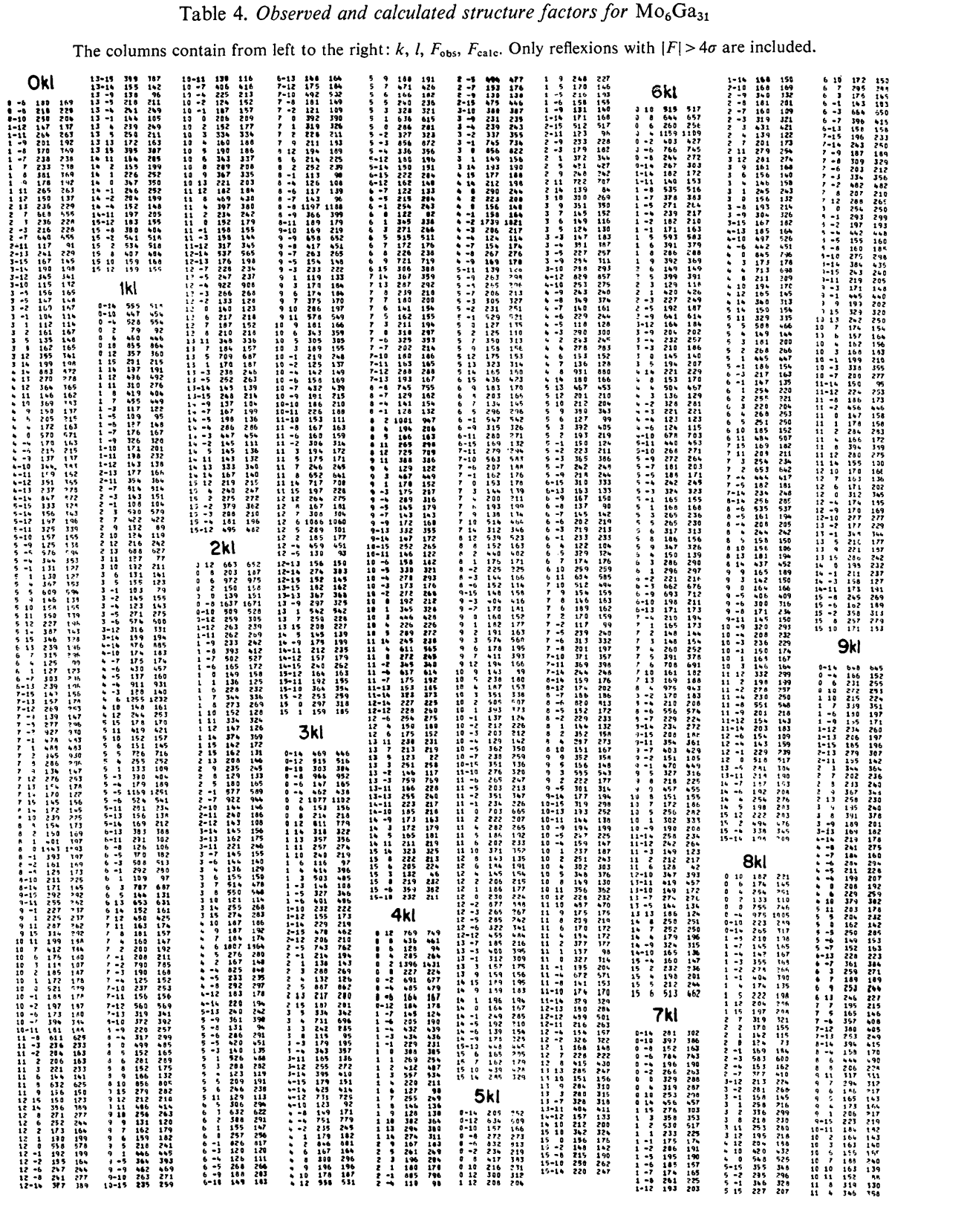

the crystal structure of a $Mo_6Ga_{31}$ single crystal has slightly different parameters from those observed with $MoGa_5$ in powder form.

### Description of the structure and discussion

The most prominent features of this crystal structure are its 28 building blocks. Each Mo atom is surrounded by 10 Ga atoms, forming different $MoGa_{10}$ polyhedra of very similar shape and size [Fig. 2(*a*)]. Such $TB_{10}$ polyhedra (T = Transition metal, B = Al, Ga) are common in B-metal-rich transition-metal compounds (Table 5) and represent a compromise between two different tendencies in these structures: the tendency of forming $TB_{12}$ icosahedra and of forming $TB_8$ cubes. In fact these $TB_{10}$ polyhedra consist of exactly one half of an icosahedron and one half of a cube, reflecting exactly therefore the 'structure equation':

$$\tfrac{1}{2}TB_{12}+\tfrac{1}{2}TB_8=TB_{10}\,. \qquad (1)$$

These building blocks in $Mo_6Ga_{31}$ are arranged in such a way that the molybdenum atoms at the centres occupy vertices of a cubic lattice that is monoclinically distorted. The arrangement of $TB_x$ polyhedra on a b.c.c. lattice is not uncommon in complex intermetallic phases containing Al or Ga. In fact, the structures of $CrGa_4$ and $MoAl_{12}$ contain building blocks that form precisely a b.c.c. structure. In the case of $CrGa_4$ the building blocks are simple Ga cubes, centred on Cr, and in $MoAl_{12}$ the building blocks are Al icosahedra, centred on Mo atoms. The same structural principle may be found in even larger structures like $Mg_{32}(Zn,Al)_{49}$ (Bergman, Waugh & Pauling, 1957), where complex arrangements of Friauf polyhedra of composition $T_xB_{113-x}$ also occupy the sites of a b.c.c. lattice.

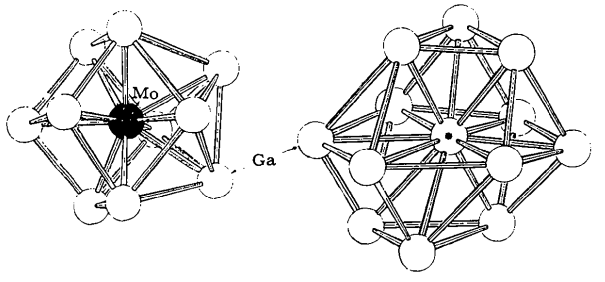


(*a*) (*b*)

Fig. 2. (*a*) Coordination polyhedron $TB_{10}$ for Mo(1), Mo(2), Mo(3), Mo(4), Mo(5) and Mo(6). (*b*) Coordination polyhedron $(T,B)B_{12}$ for Ga(26).

Table 5. *List of structure types of intermetallic compounds containing* $TB_8$, $TB_{10}$ *and* $TB_{12}$ *polyhedra*

(T = transition metal, B = Al, Ga.)

Excellent drawings of many of these structure types can be found in Schubert (1964) and Pearson (1972). Only undistorted $TB_8$ and $TB_{10}$ polyhedra are included. Many TB compounds exist with twisted $TB_8$ coordination like that in $CuAl_2$ related structures, or in $Pt_3Ga_7$ ($Ru_3Su_7$ type) or in $Ni_2Al_3$. Distorted $TB_{10}$ polyhedra also occur, like those in $V_2Ga_5$ ($Mn_2Hg_5$ type).

| | |
|---|---|
| $TB_8$ | |
| $CrGa_4$ | Schubert *et al.* (1960*a*,*b*) |
| $Mo_3Al_8$ | Pötzschke & Schubert (1962*a*) |
| $Ti_2Ga_3$ | Pötzschke & Schubert (1962*b*) |
| $Ni_3Ga_4$ | Ellner *et al.* (1969) |
| $Os_2Al_3$, $OsAl_2$ | Edshammar (1965) |
| $PtAl_2$ | Schubert (1964) |
| $TB_{10}$ | |
| $Mn_4Al_{11}$ | Bland (1958) |
| $MnAl_6$ | Nicol (1953) |
| $WAl_4$ | Bland & Clark (1958) |
| $FeAl_3$ | Black (1955) |
| $Pt_8Al_{21}$ | Edshammar (1966) |
| $Fe_2Al_5$ | Schubert & Kluge (1953) |
| $Mo_6Ga_{31}$ | This work |
| $TB_{12}$ | |
| $MoAl_{12}$ | Adam & Rich (1954) |
| $VAl_{10}$ | Brown (1957) |
| $V_7Al_{45}$ | Brown (1959) |

In the case of $MoGa_5$, however, there exists a peculiar singularity among the $MoGa_{10}$ polyhedra: one polyhedron [Fig. 2(*b*)] is distorted to such an extent

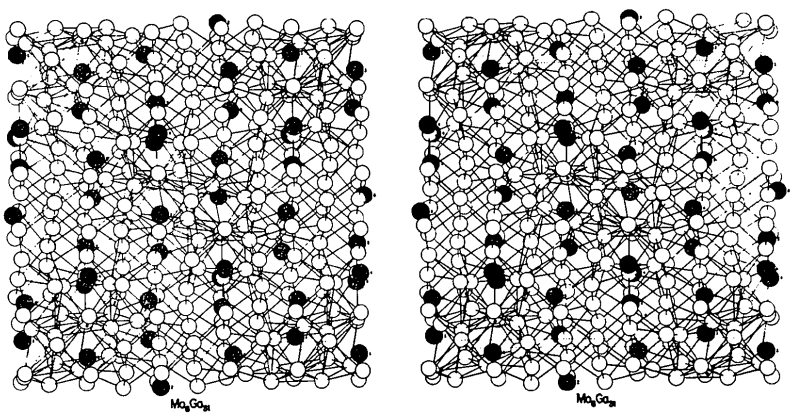

Fig. 3. Stereo drawing of $Mo_6Ga_{31}$. The centre atom Ga(26) of the $TB_{12}$ polyhedron is marked by an asterisk.

that two more Ga atoms join the shell surrounding the centre atom. In this polyhedron the centre atom is 12-fold coordinated and the atoms are approximately cubic close packed. It is the same polyhedron that has probably a gallium atom at its centre, replacing the expected Mo atom and offering some explanation for the domain of homogeneity in the $MoGa_5$ phase. Another structural feature worth mentioning is well developed layers consisting of squares of Ga atoms. They form in many different directions but do not penetrate the entire unit cell, as can be seen in the stereo drawing in Fig. 3, made using the computer program of Johnson (1965). It is interesting to see how these Ga layers themselves build up cages containing several $MoGa_{10}$ polyhedra.

All these features, but especially the very tightly packed Ga cages around the Mo atoms, can be useful in the interpretation of the anomalous magnetic behaviour of this superconductor. They may also give some clue to the interpretation of the curious behaviour of the melt at temperatures close to the solidification point. In fact it is quite conceivable that $MoGa_{10}$ clusters form already in the liquid and that the change to the lower coordination number decreases the density of the melt. X-ray diffraction on the melt should allow this point to be clarified.

*Interatomic distances in* $Mo_6Ga_{31}$

The interatomic distances for the seven independent building blocks of $Mo_6Ga_{31}$ are listed in Table 3 [computer program: *ORFFE*3, Busing *et al.* (1971*a*)].

The most striking result is the fact that this structure, like many other complex alloy structures, does not exhibit characteristic values for interatomic distances. On the contrary, $Mo_6Ga_{31}$ shows a great variety of next-neighbour distances, ranging from 2·54 to 2·93 Å for Mo–Ga bonds and from 2·66 to 3·35 Å for Ga–Ga contacts. Although these variations are quite important, one nevertheless finds certain 'mean values' remaining remarkably constant. This is especially true for the mean value of the Mo–Ga distances within one polyhedron whose observed value is around 2·63 (2) Å for all $MoGa_{10}$ polyhedra in the structure. It is interesting, therefore, to try to compare this value with the one predicted by the resonating valence-bond theory (Pauling, 1951, 1960).

The relation

$$r_{(1)} - r_{(n)} = 0{\cdot}30 \log n \qquad (2)$$

allows one to correct the single-bond metallic radii for their respective bond number $n$ in intermetallic compounds. In order to do this, one assumes that the electronic structure of the compound is closely similar to the structure of the two metals and one makes some assumptions about the valency of the ligand atoms. If one assumes molybdenum to have a valency of 6 in $Mo_6Ga_{31}$, the 10 gallium ligands have bond number $n = \frac{3}{5}$. The correction, $-0{\cdot}6 \log \frac{3}{5}$, is therefore equal to 0·133. This gives a total predicted bond distance of 2·674 Å for the Mo–Ga distances.* This value is higher than the observed mean value of 2·63 Å.

If one assigns molybdenum a valency of 7, one obtains 2·634 Å as a predicted value, which comes very close to the experimental value. This should not be interpreted, however, as supporting a valency of 7 for Mo in this compound. More likely is an electron transfer affecting the Mo–Ga distances. Present X-ray data do not permit one to detect such a transfer, although refinement of the occupancy factors (Table 2) seems to indicate that Mo may be an electron *donor*. This would contradict Raynor's hypothesis, transition metals *absorbing* electrons in aluminides (Pratt & Raynor, 1951).

The Ga–Ga distances are systematically longer than those between Mo and Ga or those observed in pure gallium. They vary over an even wider range, and no attempt was made to apply formula (2). It seems very unlikely at the moment that any theory of chemical bonding allows one to predict from first principles variations in interatomic distances of this magnitude, let alone other structural details of $Mo_6Ga_{31}$.

The author thanks Professor E. Parthé for his interest and stimulating criticism as well as Professor M. Peter for initiating this study.

* $r_{Ga} = 1{\cdot}245$, $r_{Mo} = 1{\cdot}296$ Å.

## References


ADAM, J. & RICH, J. B. (1954). *Acta Cryst.* **7**, 813–816.

BAUER, E., NOWOTNY, H. & STEMPFL, A. (1953). *Mh. Chem.* **84**, 692–700.

BERGMAN, G., WAUGH, J. L. T. & PAULING, L. (1957). *Acta Cryst.* **10**, 254–259.

BLACK, P. J. (1955). *Acta Cryst.* **8**, 175–182.

BLAND, J. A. (1958). *Acta Cryst.* **11**, 236–244.

BLAND, J. A. & CLARK, D. (1958). *Acta Cryst.* **11**, 231–244.

BORNAND, J. D., SIEMENS, R. E. & ODEN, L. L. (1973). *J. Less-Common Met.* **30**, 205–209.

BROWN, P. J. (1957). *Acta Cryst.* **10**, 133–135.

BROWN, P. J. (1959). *Acta Cryst.* **12**, 995–1002.

BURGI, H. B. & DUNITZ, J. D. (1971). *Acta Cryst.* A**27**, 117–119.

BUSING, W. R., MARTIN, K. O., LEVY, H. A., BROWN, G. M., JOHNSON, C. K. & THIESSEN, W. A. (1971*a*). *ORFFE*3. Oak Ridge National Laboratory, Oak Ridge, Tennessee.

BUSING, W. R., MARTIN, K. O., LEVY, H. A., ELLISON, R. D., HAMILTON, W. C., IBERS, J. A., JOHNSON, C. K. & THIESSEN, W. E. (1971*b*). *ORXFLS*3. Oak Ridge National Laboratory, Oak Ridge, Tennessee.

EDSHAMMAR, L. E. (1965). *Acta Chem. Scand.* **19**, 871–874.

EDSHAMMAR, L. E. (1966). *Acta Chem. Scand.* **20**, 2683–2688.

ELLNER, M., BEST, K. J., JACOBI, H. & SCHUBERT, K. (1969). *J. Less-Common Met.* **19**, 294–296.

FISCHER, Ø. H. (1972). *Helv. Phys. Acta*, **45**, 330–397.

FISCHER, Ø. H., JONES, H., BONGI, G., FREI, C. & TREYVAUD, A. (1971). *Phys. Rev. Lett.* **26**, 305–308.

HAUPTMAN, H. (1964). *Acta Cryst.* **17**, 1421–1433.

HAUPTMAN, H. & KARLE, J. (1959). *Acta Cryst.* **12**, 846.

*International Tables for X-ray Crystallography* (1962). Vol. III. Birmingham: Kynoch Press.
JACCARINO, V. & PETER, M. (1962). *Phys. Rev. Lett.* **9**, 290–292.
JOHNSON, C. K. (1965). *ORTEP*. ORNL-3794, Oak Ridge National Laboratory, Oak Ridge, Tennessee.
MAIN, P., WOOLFSON, M. M. & GERMAIN, G. (1972). *LSAM: A System of Computer Programs for the Automatic Solution of Centro-Symmetric Crystal Structures*. Dept. of Physics, Univ. of York, York, England and Laboratoire de Chimie Physique, Université de Louvain, 39 Schapenstraat, Leuven, Belgium.
MATTHIAS, B. T., COMPTON, V. B. & CORENZWIT, E. (1961). *J. Phys. Chem. Solids*, **19**, 130–133.
MEULENAER, J. DE & TOMPA, H. (1965). *Acta Cryst.* **19**, 1014–1018.
NICOL, A. D. I. (1953). *Acta Cryst.* **6**, 285–293.
PAULING, L. (1951). *Acta Cryst.* **4**, 138–140.
PAULING, L. (1960). *The Nature of the Chemical Bond*, p. 256. Ithaca: Cornell Univ. Press.
PEARSON, W. B. (1972). *The Crystal Chemistry and Physics of Metals and Alloys*. New York: Wiley–Interscience.
PÖTZSCHKE, M. & SCHUBERT, K. (1962*a*). *Z. Metallk.* **53**, 474.
PÖTZSCHKE, M. & SCHUBERT, K. (1962*b*). *Z. Metallk.* **53**, 548.
PRATT, J. N. & RAYNOR, G. V. (1951). *Proc. Roy. Soc.* A**205**, 103.
ROGERS, D. & WILSON, A. J. C. (1953). *Acta Cryst.* **6**, 439–449.
SCHUBERT, K. (1964). *Kristallstrukturen zweikomponentiger Phasen*. Berlin: Springer.
SCHUBERT, K., ANANTHARAMAN, T. R., ATA, H. O. K., MEISSNER, H. G., PÖTZSCHKE, M., ROSSTEUTSCHER, W. & STOLZ, E. (1960*a*). *Naturwissenschaften*, **47**, 512.
SCHUBERT, K., BLAU, S., BURKHARDT, W., GOHLE, R., MEISSNER, H. G., PÖTZSCHKE, M. & STOLZ, E. (1960*b*). *Naturwissenschaften*, **47**, 303.
SCHUBERT, K. & KLUGE, M. (1953). *Z. Naturforsch.* **8**a, 755.
TOMPA, H. & ALCOCK, N. W. (1969). Absorption correction program (Sept. 1969 version), link of X-RAY 67 system.
WOOLFSON, M. M. (1970). *An Introduction to X-ray Crystallography*, p. 290. Cambridge Univ. Press.
YVON, K., JEITSCHKO, W. & PARTHÉ, E. (1969). *A Fortran IV Program for the Intensity Calculation of Powder Patterns*. Laboratoire de Cristallographie aux Rayons X, Université de Genève, Switzerland.

*Acta Cryst.* (1974). B**30**, 861

# A Contribution to the Sm–Co Phase Diagram

BY Y. KHAN

*Institut für Werkstoffe der Elektrotechnik, Ruhr Universität, Bochum, Germany (BRD)*

(*Received* 14 *September* 1973; *accepted* 22 *November* 1973)

The Co-rich part of the Sm–Co system has been investigated by X-ray diffraction, metallographic and thermoanalytic methods. The existence of five closely related compounds ($Sm_2Co_7$, $SmCo_{5-x}$, $SmCo_5$, $SmCo_{5+x}$ and $Sm_2Co_{17}$) has been confirmed. A tentative phase diagram of the Co-rich part of the Sm–Co system is presented. The practical difficulties encountered in the construction of this phase diagram are discussed.

## Introduction

Since the discovery that permanent magnets with large coercivity, remanence and energy-product can be prepared on the basis of the $SmCo_5$ intermetallic compounds, many versions of the phase diagram of the binary Sm–Co system have been presented (Lihl, Ehald, Kirchmayr & Wolf, 1969; Buschow & Van der Goot, 1968; Naastepad, Den Broeder & Klein-Wassink, 1973). Recently, however, two new phases, $SmCo_{5-x}$ (a phase variant of the $CaCu_5$-type structure) (Khan & Feldmann, 1973) and $SmCo_{5+x}$ (of the $TbCu_7$-type structure) (Khan, 1974), have been reported to exist in this binary system. Even in the most recent phase diagram of the Sm–Co system (Buschow & Den Broeder, 1973), these two phases are missing. Investigations were therefore carried out in order to amend the Sm–Co phase diagram.

## Experimental

The alloys in the composition-range $Sm_2Co_7$ to $Sm_2Co_{17}$ were prepared in two series. For the first series, the alloys (1–3 g) were arc-melted on a water-cooled copper hearth under an atmosphere of specially purified argon gas (10–15 ppm oxygen). The elements were supplied by HEK (Lübeck) and had the reported purity 99·9 and 99·999 wt.% for Sm and Co respectively. The second series of alloys was prepared by casting the Sm–Co alloys (weighting about 100–150 g) in copper dies cooled by liquid nitrogen in a Balzer's medium frequency induction oven. The elements for this series were supplied by Th. Goldschmidt (Essen) and had the purity of 99·9 wt.% for both the elements.

The alloys were investigated in the as-cast state as well as after annealing at temperatures between 500 and 1400 °C (depending upon the composition of the alloy)